Available online at www.sciencedirect.com
ScienceDirect
Trans. Nonferrous Met. Soc. China 25(2015) 2948−2957
Transactions of Nonferrous Metals Society of China
www.tnmsc.cn

Texture evolution and recrystallization behaviors of Cu−Ag alloys subjected to cryogenic rolling

Yue LU, Ru MA, Yi-nong WANG

School of Materials Science and Engineering, Dalian University of Technology, Dalian 116024, China

Received 27 November 2014; accepted 30 January 2015

Abstract: The texture evolution and mechanical properties of Cu−Ag alloys subjected to severe plastic deformation at cryogenic temperature (CT) were investigated and the sequent annealing behaviors were also studied. Compared with the sheets rolled at room temperature (RT) showing copper texture, the CT-rolled sheets exhibited brass texture which indicated that cross-slip was suppressed at CT, and both the ultimate tensile strength and yield strength of the sheets were increased. Due to the in-situ recrystallization mechanism, recrystallization textures in as-annealed CT-rolled sheets were randomly distributed, while the as-annealed RT-rolled sheets mainly contained cube texture. Microstructures of the rolled and annealed sheets were observed using optical microscopy and electronic back-scatter diffraction. The results show that the dynamic recovery was suppressed during CT-rolling and resulted in higher deformation energy storage. Therefore, the recrystallization of CT-rolled sheets could start at a lower temperature than that of RT-rolled sheet at the same reduction.

Key words: cryogenic rolling; copper alloy; texture evolution; recrystallization behavior

1 Introduction

Recently, there is a great interest in bulk ultrafine grained (UFG) materials due to its excellent mechanical properties and good plasticity [1]. And several severe plastic deformation (SPD) techniques are considered the effective methods for fabricating such materials [2−4]. However, UFG materials produced by SPD usually have high strength but disappointingly low ductility [5]. Previous numerous investigations showed that high strain rate or low deformation temperature could provide high strength without decrease in ductility [6]. Accordingly, we have developed a new process, SPD at the cryogenic temperature (CT). For example, according to WANG et al [6], pure copper with high strength and ductility was obtained by deforming at liquid nitrogen temperature and followed by annealing. On the other hand, the CT rolling has been applied to the commercial Al and its alloys which can refine the grains in the materials with less plastic deformation than other SPD process [7−9].

It is well known that dislocation slip and twinning are two main plastic deformation modes in the face-centered cubic (FCC) metals, and when the materials were deformed at lower temperature, the dislocation manipulation and rearrangement would be suppressed, at this time, the deformation twinning would play an important role in carrying plastic strain [10], the twin boundary (TB) as a special kind of coherent boundary is also a barrier for dislocation slipping like the conventional GBs [11].

To date, most researches of SPD processing on pure Cu and its alloy mainly focus on the structure characterizations and mechanical properties [12−14], but the annealing behaviors of Cu alloy have not received much attention. Accordingly, accurate understanding of micromechanical behavior is a prerequisite for development and successful application of the materials whose texture evolution is closely linked to their featured deformation mechanism and microstructure [15,16]. In the view of above, in the present work, cryogenic rolling was carried out on Cu−Ag alloy to study the texture evolution and mechanical properties, and the subsequent annealing behaviors of the rolled materials were also investigated, providing the fundamental understanding

Foundation item: Project (51271046) supported by the National Natural Science Foundation of China
Corresponding author: Yi-nong WANG; Tel: +86-411-84708441; E-mail: wynmm@dlut.edu.cn
DOI: 10.1016/S1003-6326(15)63921-8

of the micromechanics of deformation texture evolutions in FCC materials, which is helpful for easy to scale up for industrial production to produce bulk ultrafine grained (UFG) alloys.

2 Experimental

The material used in this study was a commercial Cu−0.1Ag alloy which was received in the form of cold-draw bar of 10 mm in diameter. Before rolling, the Cu−Ag alloy bars were annealed at 500 °C for 1 h to obtain homogeneous microstructures and diminish the effect of mechanical processing. The rolling processes were conducted on the Cu−0.1Ag alloy bars at cryogenic temperature and room temperature (RT), respectively, and the rolling direction was parallel to the axis of the bar. The total reduction of the samples was 90% overall the thickness (diameter) with per pass of ~10% in thickness. During the CT-rolling, the samples were cooled by dipping into the liquid nitrogen prior to each rolling pass. To investigate the effect of temperature on the annealing behaviors, both the CT-rolled and RT-rolled sheets were annealed at the temperatures of 150− 400 °C for 1 h, respectively.

The optical microstructures of the rolled and as-annealed sheets were observed by standard metallographic technique after polishing and etching at room temperature using a solution of iron nitrate and ethanol (the volume ratio was 1:10) for 2 min. The microhardnesses of the as-annealed sheets were measured on a MVC−1000B tester at a load of 500 g for 15 s, and all samples were selected at least 5 points to test. Tensile specimens of dog-bone geometry with 30 mm in gauge length and 6 mm in width were cut along the planes coinciding with the rolling direction. Then, uniaxial tensile tests were carried out along the rolling direction with initial strain rate of 10^{-3} s^{-1} at room temperature. The evolutions of the textures during rolling and annealing were studied at the center layer of sheets by performing X-ray texture analysis. The {111}, {200} and {220} pole figures were measured up to a tilt angle of 70° using the Schultz reflection method and orientation distribution function (ODF) was calculated. In addition, the microstructures of individual grains in as-annealed samples were analyzed by electron back-scattering diffraction (EBSD), and the samples preparation for EBSD consisted of mechanical grinding, followed by mechanical polishing, and then electrolytically polishing in a solution of 70% orthophosphoric acid in water at −10 °C with an applied potential 2 V. EBSD was performed at 20 kV, 15 mm working distance, a tilt angle of 70°, a scan step of 0.8−1 μm and a magnification of 2000.

3 Result and discussion

3.1 Texture evolutions of rolled sheet

Rolling textures in FCC materials may include the cube {100}⟨100⟩, Goss {011}⟨100⟩, brass {011}⟨211⟩, S {123}⟨412⟩ or copper {112}⟨111⟩ texture components [17]. To facilitate the analysis of the texture characteristics of the Cu alloys, a list of the Miller indices and Euler angles of the main texture components for FCC materials after rolling are shown in Table 1. The rolling temperature and stacking fault energy (SFE) are known to have a strong influence on the development of texture during cold rolling [18]. High SFE materials (including copper) usually do not deform by twinning, which exhibit the copper-type texture. Low SFE materials that can typically deform by twinning favor the formation of a brass-type texture. The ODFs calculated from the {111}, {200} and {220} pole figures of the original and rolled sheets are exhibited in Fig. 1.

Table 1 Euler angles and Miller indices of main texture components in FCC metal

Rolling texture	Miller indice	Euler angles φ_1, Φ, φ_2/(°)
Cube	{001}⟨100⟩	0, 0, 0/90
Goss	{110}⟨100⟩	0, 45, 0
Brass	{011}⟨211⟩	35, 45, 0
Copper	{112}⟨111⟩	90, 35, 45
S	{123}⟨634⟩	61, 34, 64

From the results presented in Fig. 1(a), it can be seen that the Goss and cube textures were the major components in the original materials which also contained a small volume of copper texture. This is reasonable because the initial Cu−0.1Ag alloy was a cold-draw bar and was subjected to partially annealing prior to rolling. After CT-rolling, the sheet showed significant deformation textures with strong S and brass texture components (Fig. 1(b)) which are the stable texture components of FCC materials [19], and a weak copper texture, the original Goss and cube texture components completely disappeared. For comparison, the ODFs of the sheet deformed by RT-rolling are shown in Fig. 1(c). The major texture components were the Goss and S texture components, intensity of texture increased somewhat with reduction, the copper component decreased markedly, and a small amount of cube texture, i.e., the original texture, still could be observed which suggested that the deformation was incomplete. In addition, the volume fractions of texture components in the two rolled sheets were calculated as shown in Fig. 1(d), the fraction of brass texture increased

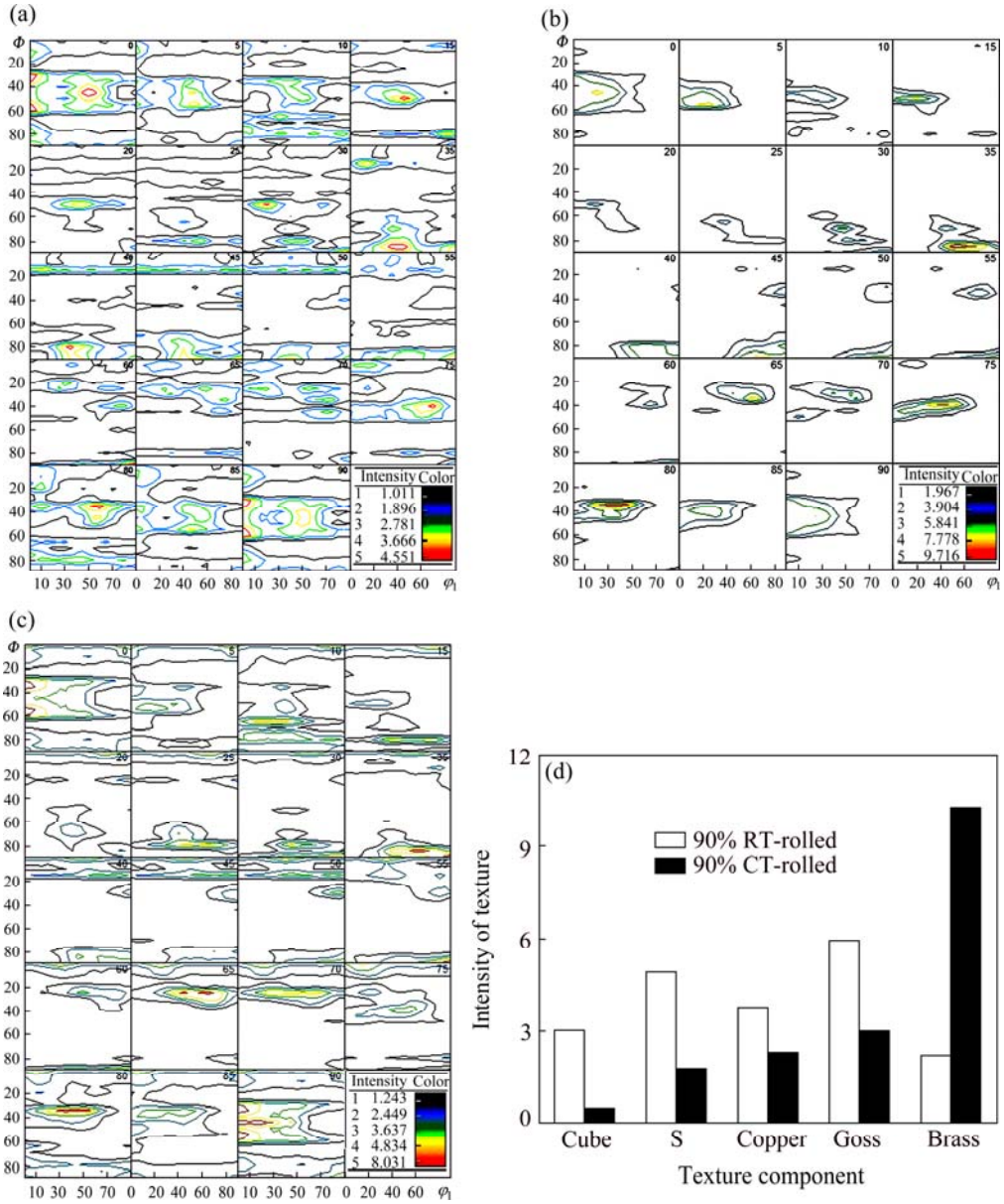

Fig. 1 ODFs of original sample (a), CT-rolled sheet (b), RT-rolled sheet (c) and evolution of rolling texture components (d)

at CT-rolling, the cube component decreased markedly. The texture results contrasted with that typically observed in materials after RT-rolling.

This effect can be ascribed to the fact that brass texture is known as a typical texture of twinning in materials, so it can be speculated that the cross-slip was suppressed while the twinning was promoted at low temperature during CT-rolling. What's more, the previous study had demonstrated that with the decrease of the deformation temperature, the copper texture would transform into brass texture through S texture [20], and this is why a strong S texture also can be observed in the CT-rolled sheet. In other words, S component seems to be the transition phase while increases the twinning. Those types of texture are often attributed to mechanical twinning which means that a great deal of twins were formed in the materials.

3.2 Mechanical properties of rolled sheet

The tensile engineering stress−strain curves of the CT-rolled and RT-rolled samples obtained from the average of several tensile test results were different with each other, as shown in Fig. 2. And the corresponding data, i.e., the yield strength (YS) and ultimate tensile strength (UTS), are listed in Table 2. As shown in the figure and table, the UTS of the sheets deformed by CT-rolling increased from 272 to 482 MPa (nearly 77% increase) after being deformed 90% in thickness, and was much higher than that of RT-rolled sheets with a UTS of 467 MPa.

The drastic increase of UTS and YS with the strain implies that dynamic recovery was effectively

suppressed during CT-rolling, and due to the suppression of dislocation cross-slip and climb, twinning was activated.

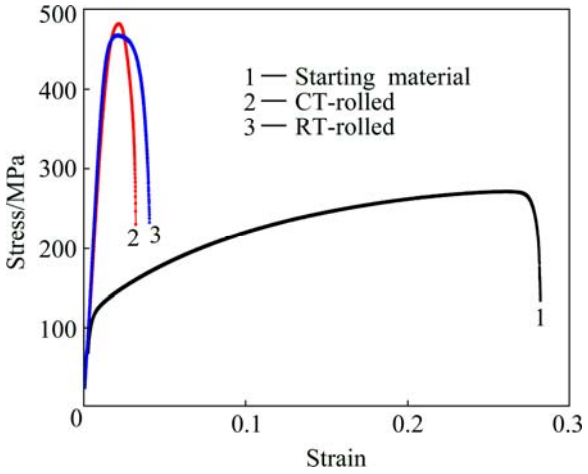

Fig. 2 Tensile stress−strain curves of samples before and after rolling

Table 2 Mechanical properties of alloys subjected to different conditions

Alloy	UTS/MPa	YS/MPa
Original	272	112
90% CT-rolled	482	472
90% RT-rolled	467	452

3.3 Microstructure characteristics of rolled sheet after annealing

Figure 3 shows the optical microstructures of the rolled sheets after annealing at 300 and 400 °C for 1 h, respectively. The RT-rolled sheet after annealing at 300 °C, no recrystallized microstructure was found in both RT-rolled sheet and CT-rolled sheet. Despite this, the recrystallized microstructure can be observed clearly in the coarse grains of the CT-rolled sheet after annealing at 300 °C, while in the as-annealed RT-rolled sheet, the recrystallized microstructure only can be observed at 400 °C. The microstructures of CT-rolled sheet after annealing at 400 °C exhibited equiaxed grains with the size of 10−15 μm and contained a lot of annealing twins distributed in the coarse grains.

The microstructures of the rolled sheet annealed at 300 and 400 °C for 1 h were also observed by the EBSD orientation maps, as shown in Fig. 4. In these images, the red lines used to characterize the $\Sigma 3$ twin boundaries, while the black lines denote the high angle boundaries (>15°), and other color lines represent some special boundaries ($3<\Sigma<27$). After annealing at 300 °C, the recrystallizations occurred in local areas of the CT-rolled sheet (Fig. 4(a)), whereas the RT-rolled sheet still exhibited the deformed microstructure (Fig. 4(b)). As annealed at 400 °C, there has been little difference between the two rolled sheets.

At a low deformation temperature, the dislocation cross-slip would be suppressed, while the deformation

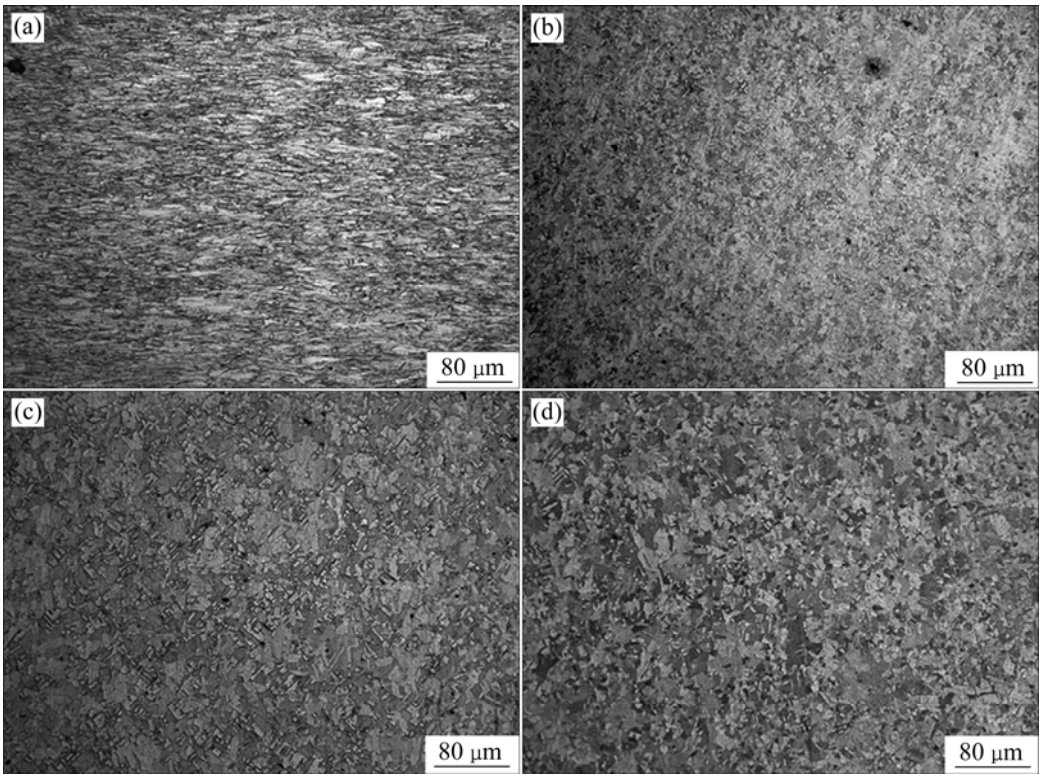

Fig. 3 OM images of rolled sheets after annealing at 300°C and 400 °C: (a, b) RT-rolled; (c, d) CT-rolled

twinning was increased to coordinate deformation during the CT-rolling. And the deformation twinning would provide a higher stored energy than the cross-slip, so with the increase of the twinning, the driving force for recrystallization could be increased due to more stored energy. In conclusion, the CT-rolled sheet had a higher recrystallization driving force than the RT-rolled sheet, and during annealing, the recrystallization would occur earlier in CT-rolled sheet. A comparison of the number fraction of $\Sigma 3^n$ boundaries is shown in Fig. 5. In the CT-rolled sheet, the number fraction of $\Sigma 3$ boundaries was decreased from 55.9% to 51.6%, and the $\Sigma 9$ boundaries were also decreased dramatically after annealing at 400 °C. This phenomenon suggested that a higher recrystallization driving force could be provided during CT-rolling which would result in the recrystallization in a short time and correspondingly induce the formation of the high-angle boundaries. And the high-angle boundaries would prevent the mobility of the grains.

The recrystallization fraction and hardness of the as-annealed rolled sheets are exhibited in Fig. 6. As annealed at 200 °C, both the RT-rolled and CT-rolled sheets were still marked by the deformation structure, so both had a similar recrystallization fraction with a small value, and the rolled sheets exhibited no soften behavior. However, after annealing at 300 °C, the recrystallization fraction in CT-rolled sheet grew rapidly and rose to 87%, while in the RT-rolled sheet, the value was still very small, just as 3%. This can be judged that the incubation period for recrystallization in CT-rolled sheet was very short. And correspondingly, the soften behavior occurred

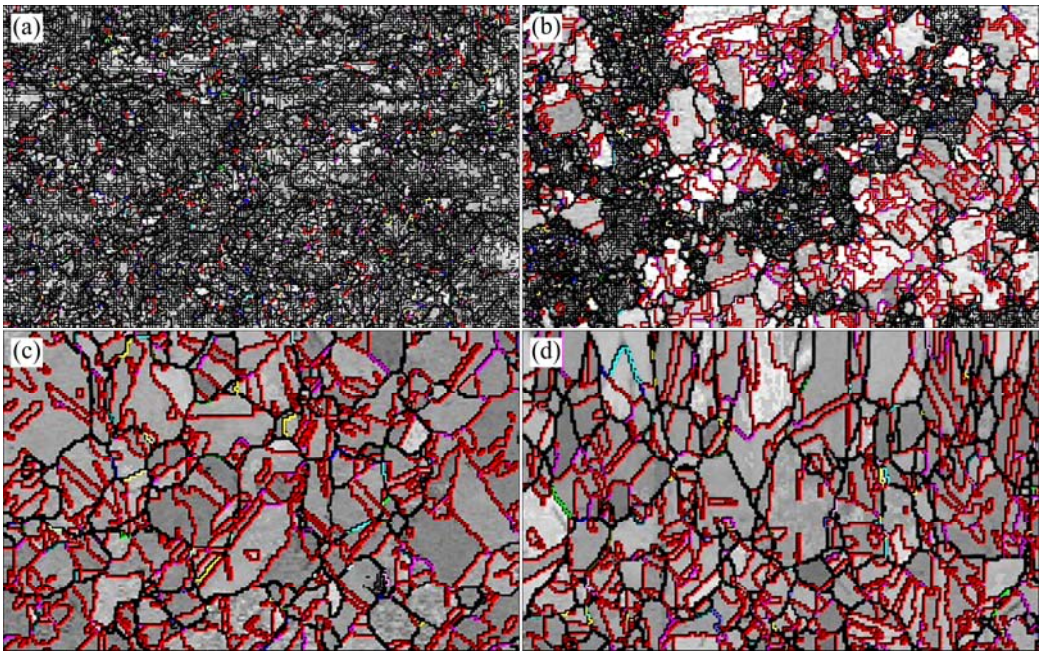

Fig. 4 EBSD orientation maps of RT-rolled sheet (a), CT-rolled sheet annealed at 300 °C (b), RT-rolled sheet (c), and CT-rolled sheet annealed at 400 °C (d)

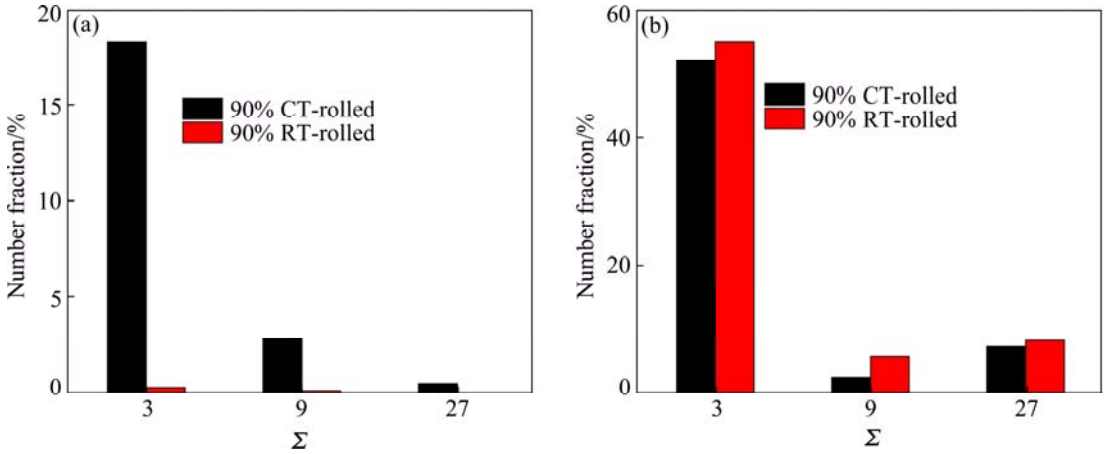

Fig. 5 Number fractions of $\Sigma 3^n$ boundaries of rolled sheet annealed at 300 °C (a) and 400 °C (b)

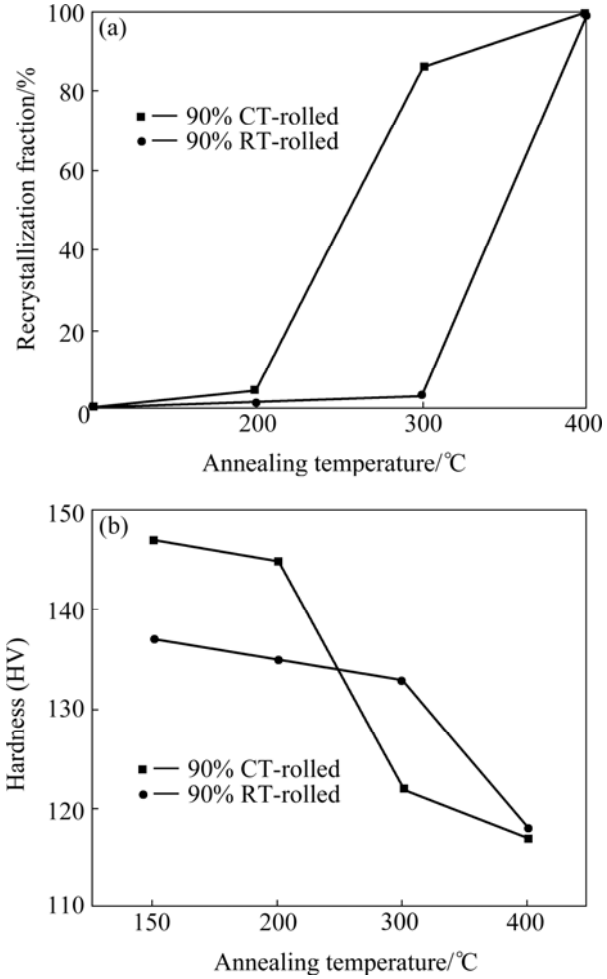

Fig. 6 Effect of annealing temperature on recrystallized volume fraction (a) and hardness (b) of rolled sheets

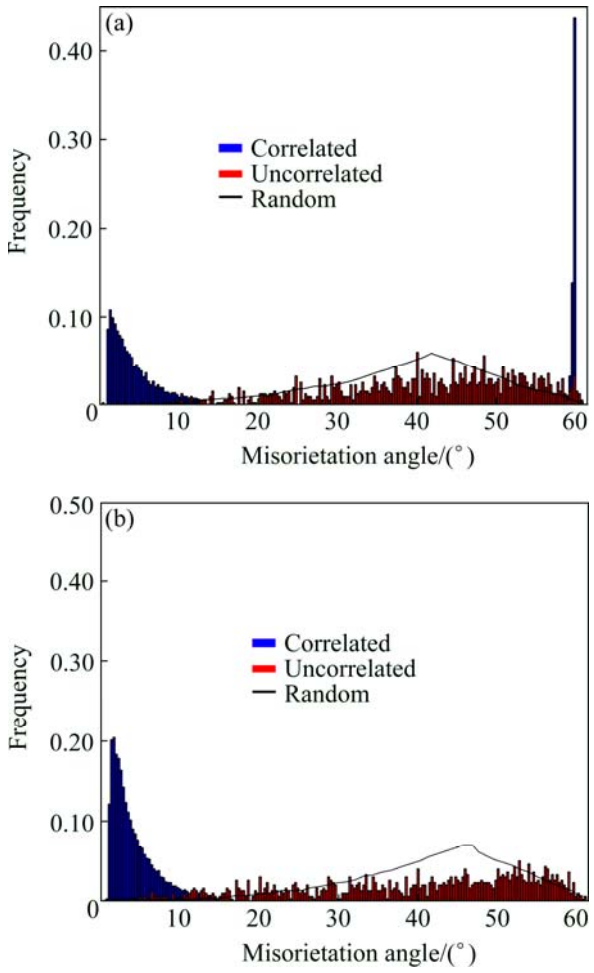

Fig. 7 Grain boundary misorientation distribution of CT-rolled sheet (a) and RT-rolled sheet (b) annealed at 300 °C

much more significantly in CT-rolled sheet than in RT-rolled sheet. After annealing at 400 °C, it can be found that the recrystallization was full completed in both rolled sheets, so the hardness of rolled sheets reached a similar value.

The grain boundary misorientation distributions of the rolled sheets annealed at 300 °C are shown in Fig. 7. It can be found that there have been a large fraction of low angle grain boundaries in the as-annealed RT-rolled sheet which indicated that the recrystallization almost did not occur. However, in the as-annealed CT-rolled sheet, there were a large fraction of high angle grain boundaries (misorientation angles above 15°), and this phenomenon was the typical recrystallization grain boundary misorientation distribution which suggested that significant recrystallization occurred in the CT-rolled sheet during annealing.

3.4 Texture features of rolled sheet after annealing

The ODFs obtained from the textures of the rolled sheet after annealing at different temperatures are given in Fig. 8. Compared with the RT-rolled sheet annealed at 200 °C which contained copper texture component in majority (Fig. 8(b)), the CT-rolled sheet annealed at the same condition presented a special texture characteristics which included the strong brass texture and Goss texture (Fig. 8(a)). Combined with the previous results, i.e., the ODF features of the rolled sheet (Figs. 1(b) and (c)), it can be concluded that both the RT-rolled and CT-rolled sheets after annealing at 200 °C retained the deformed texture characteristics, and the maximum intensity of the texture in the as-annealed CT-rolled sheet weakened from 9.7 to 7.1. After annealing at 300 °C, it can be found the appearance of the cube texture component in CT-rolled sheet, and simultaneously, the brass texture intensity was strengthened, while the intensity of the Goss texture was significantly weakened (Fig. 8(c)). However, there were no obvious changes in the texture features of the RT-rolled sheet after annealing at 300 °C (Fig. 8(d)). After annealing at 400 °C, the main texture component of the RT-rolled sheet was the cube texture

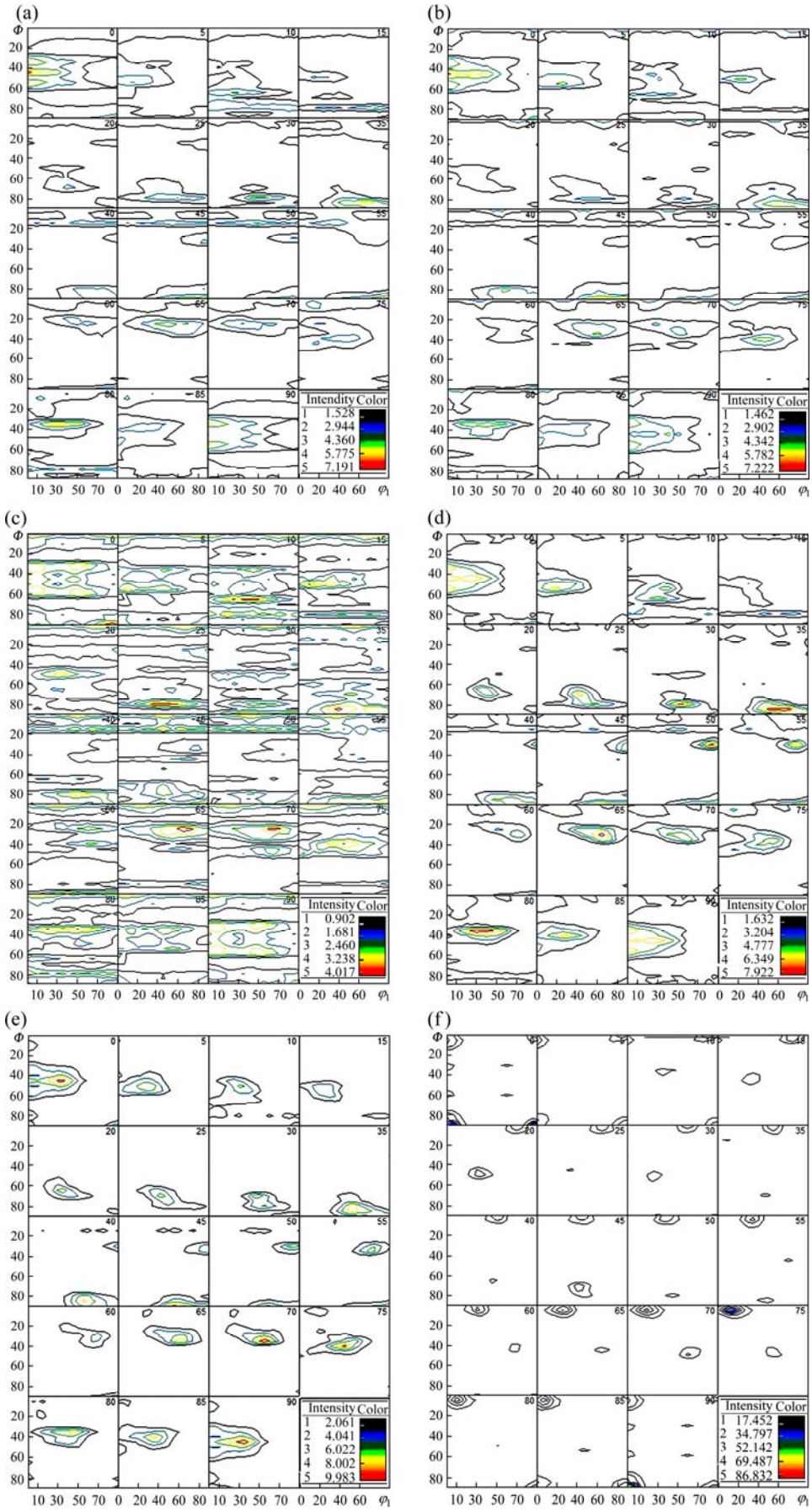

Fig. 8 ODFs of CT-rolled sheet followed by annealing at 200 °C (a), 300 °C (b), 400 °C (c) and RT-rolled sheet followed by annealing at 200 °C (d) 300 °C (e) and 400 °C (f)

with an intensity of 86.8, and all other texture components almost disappeared (Fig. 8(f)). However, in the as-annealed CT-rolled sheet, the textures were composed by Goss, brass, cube and S textures, where all components had small intensity close to 4 (Fig. 8(e)) and can be determined to be a random texture characteristic.

The annealing behaviors were also analyzed by the EBSD method. Figure 9 presented the {111} pole figures of the rolled sheets after annealing at 300 °C and 400 °C which were obtained from the EBSD data. The {111} pole figures of the CT-rolled and RT-rolled sheets annealed at 300 °C were similar with each other, and the difference between the two was that the as-annealed CT-rolled sheet exhibited some amount of cube texture (as shown in Fig. 9(a)) which indicated that the recrystallization began. From Fig. 9(b), it can be seen that after annealing at 400 °C, Goss texture turned to be the major component in CT-rolled sheet. While the {001}⟨100⟩ cube texture was the main component in RT-rolled sheet annealed at 400 °C which can be observed in Fig. 9(d). All these results were in line with the macro-texture characteristics which were presented in ODFs.

As annealed at different temperatures, the RT-rolled sheet exhibited a much stronger cube texture which can be speculated a smaller dislocation density in the materials, so it can be concluded that the RT-rolled sheet had smaller stored energies in the grains than that in the CT-rolled sheet. After annealing, the texture characteristics of CT-rolled sheet was constituted by the retained deformed rolling texture and a little cube texture, and this phenomenon can be attributed to the in-situ recrystallization mechanism which often occurs under a high recrystallization driving force [21]. Generally, the recovery is a thermally activated process, and it is often suppressed during the deformation at CT and leads to the emergence of twinning which would result in a higher dislocation density. As analyzed previously, it can be concluded that the driving force for recrystallization would be increased during CT-rolling process with the emergence of twinning, and this is another reason for the recrystallization in CT-rolled sheet starting earlier than that in RT-rolled sheet. Based on the above analysis, it also can be concluded that the recrystallization process would occur earlier in the CT-rolled sheet than in the RT-rolled sheet when annealed at the same temperature according to the previous results of the microstructure characteristics.

4 Conclusions

1) The appearance of brass and S textures which replaced the copper texture in the original materials during CT-rolling indicated that the cross-slip was

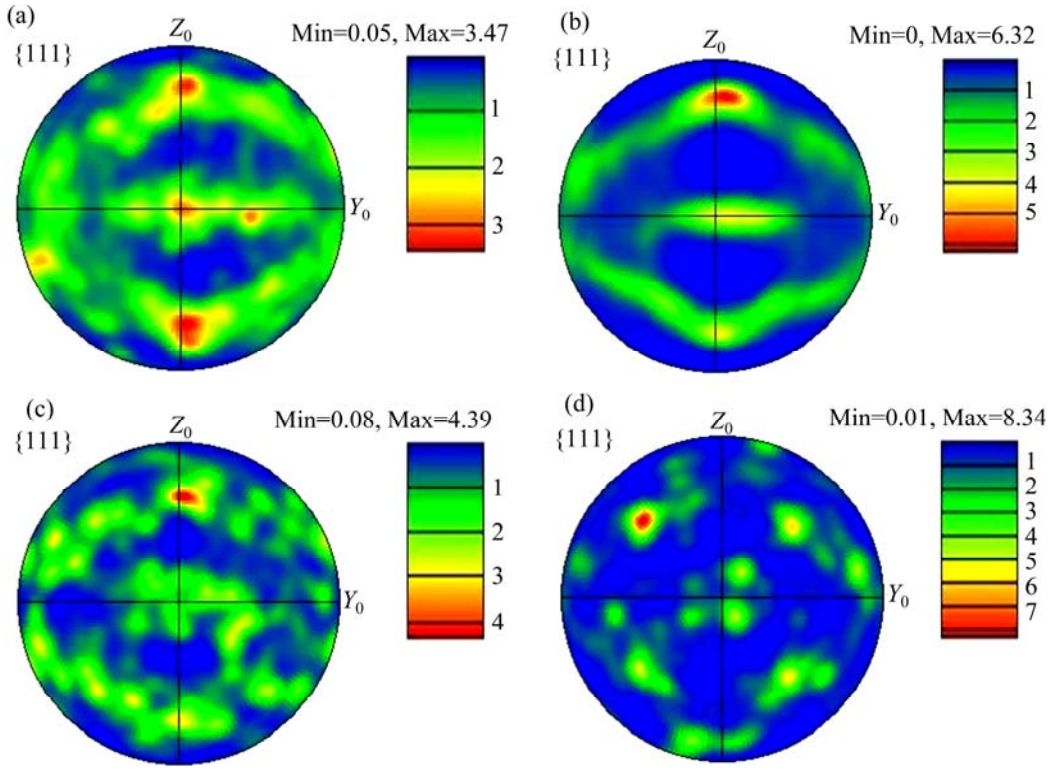

Fig. 9 {111} pole figures of CT-rolled sheet followed by annealing at 300 °C (a) 400 °C (b) and RT-rolled sheet followed by annealing at 300 °C (c), 400 °C (d)

suppressed at cryogenic temperature. Compared with the materials rolled at room temperature, it can be found that both the tensile strength and yield strength of the materials rolled at CT were increased. And this phenomenon can facilitate the formation of the mechanical twinning in the CT-rolled sheet.

2) As annealed at the temperature of 300 °C, the CT-rolled sheet was softened rapidly and much faster than the RT-rolled sheet. The main recrystallization textures in the CT-rolled after annealing at 400 °C were composed by Goss, brass, cube and S texture components and close to a random distribution, and this result was different with the as-annealed RT-rolled sheet which mainly constituted by the cube texture. This phenomenon can be attributed to the in-situ recrystallization mechanism which can result in retained rolling texture.

3) From the observation of the microstructures in annealed materials, it can be indicated that during CT-rolling, the dynamic recovery was suppressed and correspondingly a higher driving force for recrystallization than that in RT-rolling can be provided. Combined the recrystallization fraction in the samples under with different rolling conditions, it can be demonstrated that the recrystallization in the CT-rolled samples started at a lower temperature than that in the RT-rolled sheet at the same reduction of 90%.

References

[1] KONKOVA T, MIRONOV S, KORZNIKOV A, SEMIATIN S L. Microstructural response of pure copper to cryogenic rolling [J]. Acta Materialia, 2010, 58(16): 5262−5273.

[2] VALIEV R Z, ISLAMGALIEV R K, ALEXANDROV I V. Bulk nanostructured materials from severe plastic deformation [J]. Progress in Materials Science, 2000, 45(2): 103−189.

[3] HEBESBERGER T, STUWE H P, VORHAUER A, WESTSCHER A, PIPPAN R. Structure of Cu deformed by high pressure torsion [J]. Acta Materialia, 2005, 53(2): 393−402.

[4] RAO P N, KAURWAR A, SINGH D, JAYAGANTHAN R. Enhancement in strength and ductility of Al−Mg−Si alloy by cryorolling followed by warm rolling [J]. Procedia Engineering, 2014, 75: 123−128.

[5] SAN Xing-yuan, LIANG Xiao-guang, CHENG Lian-ping, SHEN Li, ZHU Xin-kun. Effect of stacking fault energy on mechanical properties of ultrafine-grain Cu and Cu−Al alloy processed by cold-rolling [J]. Transactions of Nonferrous Metals Society of China, 2012, 22(4): 819−824.

[6] WANG Y, CHEN M, ZHOU F, MA E. High tensile ductility in a nanostructured metal [J]. Nature, 2002, 419(6910): 912−915.

[7] RANGATAJU N, RAGHURAM T, KRISHNA B V, RAO P, VENUGOPAL P. Effect of cryo-rolling and annealing on microstructure and properties of commercially pure aluminium [J]. Materials Science and Engineering A, 2005, 398(1): 246−251.

[8] LEE Y B, SHIN D H, PARK K T, NAM W J. Effect of annealing temperature on microstructures and mechanical properties of a 5083 Al alloy deformed at cryogenic temperature [J]. Scripta Materialia, 2004, 51(4): 355−359.

[9] LU L, SHEN Y, CHEN X, QIAN L, LU K. Ultrahigh strength and high electrical conductivity in copper [J]. Science, 2004, 304(5669): 422−426.

[10] LI Y S, TAO N R, LU K. Microstructural evolution and nanostructure formation in copper during dynamic plastic deformation at cryogenic temperatures [J]. Acta Materialia, 2008, 56(2): 230−241.

[11] ZHANG Y, TAO N R, LU K. Mechanical properties and rolling behaviors of nano-grained copper with embedded nano-twin bundles [J]. Acta Materialia, 2008, 56(11): 2429−2440.

[12] SARMA V S, WANG J, JIAN W W, KAUFFMANN A, CONRAD H, FREUDENBERGER J, ZHU Y T. Role of stacking fault energy in strengthening due to cryo-deformation of FCC metals [J]. Materials Science and Engineering A, 2010, 527(29): 7624−7630.

[13] JIA N, EISENLOHR P, ROTERS F, RAABE D, ZHAO X. Orientation dependence of shear banding in face-centered-cubic single crystals [J]. Acta Materialia, 2012, 60(8): 3415−3434.

[14] CHOWDHURY S G, DAS S, DE P K. Cold rolling behaviour and textural evolution in AISI 316L austenitic stainless steel [J]. Acta Materialia, 2005, 53(14): 3951−3959.

[15] JIA N, ZHAO X. Study on the micromechanism of fcc metals with low stacking fault energy during cold rolling: example of alpha-brass [EB/OL]. [2012−10−17]. http://www.paper.edu.cn/releasepaper/content/201210-132.

[16] JIA N, NIE Z H, REN Y, LIN P R, WANG Y D, ZHAO X. Formation of deformation textures in face-centered-cubic materials studied by in-situ high-energy X-ray diffraction and self-consistent model [J]. Metallurgical and Materials Transactions A, 2010, 41(5): 1246−1254.

[17] BRACKE L, VERBEKEN K, KESTENS L, PENNING J. Microstructure and texture evolution during cold rolling and annealing of a high Mn TWIP steel [J]. Acta Materialia, 2009, 57(5): 1512−1524.

[18] KUMAR B R, SINGH A K, DAS S, BHATTACHARYA D K. Cold rolling texture in AISI 304 stainless steel [J]. Materials Science and Engineering A, 2004, 364(1): 132−139.

[19] MOLODOV D A, BOZZOLO N. Observations on the effect of a magnetic field on the annealing texture and microstructure evolution in zirconium [J]. Acta Materialia, 2010, 58(10): 3568−3581.

[20] KONKOVA T, MIRONOV S, KORZNIKOV A, MYSHLYAEV M M, SEMIATIN S L. Annealing behavior of cryogenically-rolled copper [J]. Materials Science and Engineering A, 2013, 585: 178−189.

[21] JENSEN D J, LAURIDSEN E M, VANDERMEER R A. In-situ determination of grain boundary migration during recrystallization [C]// Science and Technology of Interfaces, International Symposium in Honor of Dr. Bhakta Rath. New York: John Wiley & Sons, 2013: 361.

液氮低温轧制 Cu−Ag 合金的织构演变和再结晶行为

鲁 月，马 茹，王轶农

大连理工大学 材料科学与工程学院，大连 116024

摘 要：对 Cu−Ag 合金在低温下进行大变形量轧制加工，研究其织构演化特征和力学性能，随后对轧制板材进行热处理，观察其退火行为。结果表明，与常温轧制板所表现的铜型织构不同，低温下轧制板材内的交滑移机制被抑制，而其主要织构特征为黄铜型织构，且板材的抗拉强度和屈服强度均有提高。退火后，低温轧制板内发生原位再结晶，其织构随机分布，而常温轧制板的退火织构主要为立方织构。利用金相和电子背散射衍射手段观察退火前后材料的微观组织，发现低温轧制时板材内动态回复过程被抑制，因而轧制后变形储能较高，退火时，与常温轧制板相比能在较低温度发生再结晶软化行为。

关键词：液氮低温轧制；铜合金；织构演变；再结晶行为

(Edited by Yun-bin HE)